

# Subdivision of point-normal pairs with application to smoothing feasible robot path

Evgeny Lipovetsky <sup>\*†</sup>

## Abstract

In a previous paper [11] we introduced a weighted binary average of two 2D point-normal pairs, termed *circle average*, and investigated subdivision schemes based on it. These schemes refine point-normal pairs in 2D, and converge to limit curves and limit normals. Such a scheme has the disadvantage that the limit normals are not the normals of the limit curve. In this paper we solve this problem by proposing a new averaging method, and obtaining a new family of algorithms based on it. We demonstrate their new editing capabilities and apply this subdivision technique to smooth a precomputed feasible polygonal point robot path.

**Keywords:** subdivision of 2D point-normal pairs, Bezier quasi-average, 2D curve design, modified Lane-Riesenfeld algorithm, modified 4-point scheme, subdivision in environment with obstacles, robot path smoothing

## 1 Introduction

Subdivision schemes gained significant appreciation through the years. Linear subdivision schemes are thoroughly investigated and used in many applications of Computer Graphics and Computer Aided Geometric Design. The typical input for this type of schemes is a mesh of vertices. An overview of linear schemes can be found, e.g., in [8]. As the research progressed, linear schemes were adapted to other types of geometric objects such as sets of points (e.g. [7]), manifold-valued data (e.g. [14], [16]), nets of functions (e.g. [5]). Further developments consider combined types of input data, such as point-normal pairs (e.g. [3], [1], [11]) or point-tangent pairs (e.g. [17]). New types of data and algorithms require new tools and techniques for analysis (e.g [9], [12]).

In a previous paper [11] we introduced a weighted binary average of two 2D point-normal pairs (PNPs), termed *circle average*. We defined subdivision schemes based on it, which generate curves refining PNPs. A severe disadvantage of the subdivision schemes investigated in [11] is that the limit normals generated by a scheme are not the normals of the limit curve. We overcome this limitation in this paper, proposing a new averaging method while keeping our framework:

- (i) Writing a linear scheme refining points in terms of repeated linear weighted binary averages.

---

<sup>\*</sup>The contribution of Evgeny Lipovetsky is part of his Ph.D. research conducted at Tel-Aviv University.

<sup>†</sup>`evgenyl@mail.tau.ac.il`, School of Computer Sciences, Tel-Aviv Univ., Israel

- (ii) Substituting each linear weighted average of two points by our new averaging method applied to two PNPs.

The schemes obtained by the above two steps are termed *modified schemes* of the corresponding linear scheme. A further modification of these schemes is applied to smooth a precomputed robot path.

The problem of generating a smooth path under various constraints is studied extensively. For example, cubic polynomials [15] or splines [4] are used for trajectory computation of a car-like robot. In [10], a spline-based optimization is performed for a given valid polyline path, using a variant of gradient descent method. This is close to the construction presented here in the sense that a piecewise linear path is computed first and then it is smoothed by an algorithm. Our algorithm seems to be simpler.

### 1.1 Our contribution

We exploit the idea in [1] to use a Bezier curve as an auxiliary object to sample a point and a normal from. We extend this idea and come up with a new averaging method. The modified schemes with this method generate curves that lack cusps, whatever the input data is, in contrast to the scheme in [1]. We prove that the limit normals of such a converging scheme are the normals of the limit curve. A direct consequence of this result is that the limit curve is  $G^1$ .

We show the flexibility of our approach by updating the averaging method and then using it in a modified subdivision algorithm for smoothing a precomputed point robot polygonal path. To the best of our knowledge, the application of subdivision techniques to the generation of a smooth curve in an environment with obstacles is new (has not been reported in the literature).

### 1.2 Outline

After some brief preliminaries in Section 2, we introduce the new basic averaging method in Section 3, and study its properties. In Section 4, the Lane-Riesenfeld algorithm and the 4-point scheme are presented and then modified, and their editing capabilities are demonstrated.

We study the problem of smoothing a precomputed point robot polygonal path in Section 5. First, we recall a simple way to define initial normals when the initial data consists of a polyline only, and then extend the definition of the basic averaging method to avoid obstacles. In Section 5.4 we explain how we measure the smoothness of a refined polyline. Several examples with comments are given in Section 5.5. Conclusions and some directions for future work are proposed in Sections 6 and 7, respectively.

## 2 Notation

We consider a polyline that consists of  $k$  points  $\{p_i\}_{i=0,\dots,k-1}$ , with  $p_{i-1}, p_i$  the endpoints of the  $i$ -th edge. The length of the edge  $[p_{i-1}, p_i]$  is denoted by  $|p_{i-1}p_i|$ , and  $\overrightarrow{p_{i-1}p_i}$  refers the vector  $p_i - p_{i-1}$ . If  $p_0 = p_{k-1}$ , then the input polyline is a polygon. We assume that the points  $\{p_i\}_{i=0,\dots,k-1}$  are ordered clockwise. We denote  $P_i = (p_i, n_i)$  a point-normal pair with the point  $p_i$  and the normal  $n_i$  associated to  $p_i$ .

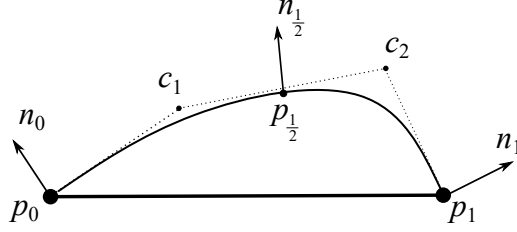


Figure 1: Computing  $P_{\frac{1}{2}}$

### 3 Bezier quasi-average

In this section we introduce a new method to average two point-normal pairs.

Given two pairs  $P_0 = (p_0, n_0)$  and  $P_1 = (p_1, n_1)$  of PNPs, we produce a new pair  $P_\omega = (p_\omega, n_\omega) = P_0 \tilde{\odot}_\omega P_1$ . We construct an auxiliary cubic Bezier curve, which interpolates the given data, and sample this curve at the parameter  $\omega$ , obtaining the average PNP,  $P_\omega = (p_\omega, n_\omega)$ .

A cubic Bezier curve is defined by its four control points  $c_i, i = 0, \dots, 3$ , and the directions of its tangent lines at the endpoints  $c_0, c_3$  are collinear with  $\overrightarrow{c_0c_1}, \overrightarrow{c_3c_2}$  respectively.

The construction of  $c_i, i = 0, \dots, 3$  is done by the following algorithm.

#### Algorithm A

1. Set  $c_0 = p_0$ , and  $c_3 = p_1$ .
2. Compute  $d_0$  as the normal  $n_0$  rotated  $\pi/2$  clockwise, and  $d_1$  as the normal  $n_1$  rotated  $\pi/2$  counter-clockwise.
3. Let  $\theta$  be the angle between the normals  $n_0$  and  $n_1$ . Compute

$$\ell = \frac{|p_0p_1|}{3 \cos^2 \frac{\theta}{4}} \quad (1)$$

4. Set  $c_i = p_{i-1} + \ell d_{i-1}, i = 1, 2$ .
5. Sample the Bezier curve defined by  $c_i, i = 0, \dots, 3$  at the parameter  $\omega$ , to obtain  $p_\omega, n_\omega$ .

Note that  $(p_\omega, n_\omega)$  is not an average since it depends on the order of the two PNPs. Also, the presented method lacks the consistency property typical to the linear average, and satisfied by the circle average [11], namely

$$\forall t, s, k \in [0, 1], (P_0 \odot_t P_1) \odot_k (P_0 \odot_s P_1) = P_0 \odot_{\omega^*} P_1, \omega^* = ks + (1 - k)t. \quad (2)$$

The consistency property (2) "almost holds" in the special case when  $P_0, P_1$  are sampled from a circle. The term "almost holds" regards the approximation quality of a circle by a Bezier curve with the choice (1) for the length of tangents

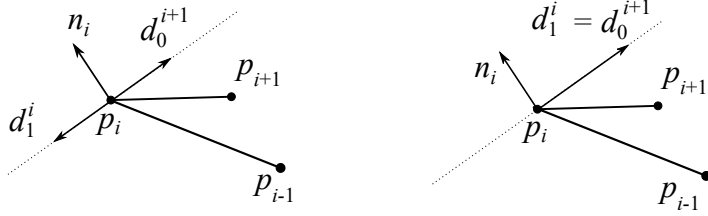


Figure 2: Two ways to rotate a normal of a PNP: considering the order of the neighbor vertex (left), considering the geometry of the neighbor segments (right).

[6]. Therefore we term the procedure of Algorithm A a quasi-averaging method, and its output *Bezier quasi-average* (BQA).

A generic example is shown in Figure 1. Two aspects of this method are motivated by circle reconstruction: the rotation directions of the normals and the tangent lengths.

The normals are rotated by  $\pi/2$  to obtain tangent directions. The most important aspect in the rotation decision (clockwise vs. counter-clockwise) is that the rotation directions are different, and they do not depend on geometric properties (like some kind of projection of  $[p_0, p_1]$  on  $d_0$  ( $d_1$ ), for example). Otherwise, cusps may occur at the points of the refined polyline.

Consider two sequential edges  $[p_{i-1}, p_i]$ ,  $[p_i, p_{i+1}]$ , the  $i$ -th and the  $(i+1)$ -th segments. The line, which is perpendicular to  $n_i$  and passes through  $p_i$ , contains control points of the two auxiliary Bezier curves:  $c_1^i$  and  $c_0^{i+1}$ , corresponding to the  $i$ -th and  $(i+1)$ -th segments respectively. The decision procedure in Algorithm A defines the tangent vectors  $d_1^i$  and  $d_0^{i+1}$  in opposite directions. This might not hold if the decision is based upon the projections of  $p_{i-1}$ ,  $p_{i+1}$  on that line. See Figure 2 for an example. We chose the rotation directions above under the assumption that  $\{p_i\}_{i=0, \dots, k-1}$  are ordered clockwise.

**Remark 3.1.** *It is shown in [6] that a cubic Bezier curve approximates well a circle arc if the distances  $|c_0c_1|$  and  $|c_2c_3|$  are computed as in (1). So, if the pairs  $P_0$  and  $P_1$  are taken from a circle then  $P_\omega$  is very close to the point and normal sampled from the corresponding position on that circle. We change the definition of  $\ell$  in Section 5 to meet additional constraints.*

Important property of the construction in Algorithm A is stated in the following theorem.

**Theorem 3.2.** *The control polyline of the auxiliary Bezier curve in Algorithm A does not have self-intersections.*

*Proof.* Denote  $e = |p_0p_1|$ , and define a local coordinate system by  $p_0 = (0, 0)$ ,  $p_1 = (e, 0)$ . Denote the angle between the tangent vectors  $d_0$  and  $d_1$  and the positive direction of the  $x$ -axis as  $\alpha$  and  $\beta$  respectively. Note that  $\theta = \pi + \alpha - \beta$ . We construct two lines  $L_0, L_1$ . The line  $L_0$  ( $L_1$ ) passes through the point  $p_0$  ( $p_1$ ) in direction  $d_0$ , ( $d_1$ ). The point  $c_1$  ( $c_2$ ) is on the line  $L_0$  ( $L_1$ ). We denote by  $q$  the intersection point of these two lines. We prove by contradiction that  $d_0$  and  $d_1$  do not intersect.

Both  $|p_0q|$  and  $|p_1q|$  have to be less than  $\ell$  to make the two tangents intersect. W.l.o.g., we assume that  $q$  is in the upper half-plane, relative to the  $x$ -axis.

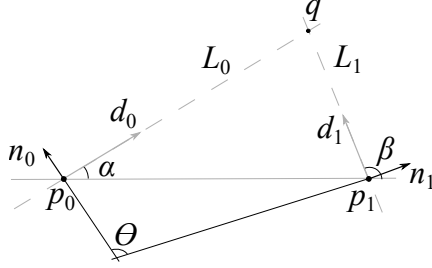


Figure 3: Setup for Theorem 3.2.

Namely, that  $0 < \alpha < \beta < \pi$ . We study the triangle  $\triangle p_0 q p_1$ . In this triangle,  $\angle q p_0 p_1 = \alpha$  and  $\angle q p_1 p_0 = \pi - \beta$ . So

$$|p_0 q| \cos \alpha + |p_1 q| \cos(\pi - \beta) = e. \quad (3)$$

Since in our construction (Algorithm A)  $|p_0 q| = |p_1 q| = \ell$ , then, in view of (1),

$$\frac{e}{3 \cos^2 \frac{\theta}{4}} (\cos \alpha + \cos(\pi - \beta)) = e. \quad (4)$$

We perform trigonometric computations on the left of (4) and get

$$\begin{aligned} \cos(\pi - \beta) + \cos \alpha &= 2 \cos \frac{\pi - \beta + \alpha}{2} \cos \left( \frac{\pi}{2} - \frac{\alpha + \beta}{2} \right) \\ &= 2 \cos \frac{\theta}{2} \sin \frac{\alpha + \beta}{2} \\ &\leq 2 \cos \frac{\theta}{4}. \end{aligned} \quad (5)$$

Inserting (5) into the left hand side of (4), and since  $0 \leq \theta \leq \pi$ , we obtain

$$\frac{e}{3 \cos^2 \frac{\theta}{4}} (\cos \alpha + \cos(\pi - \beta)) \leq \frac{2e}{3 \cos \frac{\theta}{4}} \leq \frac{2 \cdot 2}{3 \cdot \sqrt{2}} e < e. \quad (6)$$

Thus, we arrive at a contradiction, and the tangents  $d_0$  and  $d_1$  do not intersect.  $\square$

## 4 Modified subdivision schemes

We use our methodology, presented in the Introduction, to modify any linear converging subdivision scheme to refine PNPs.

To define the notion of convergence of a subdivision scheme refining point-normal pairs, we associate with the pairs  $\{P_i^j = (p_i^j, n_i^j)\}_{i \in \mathbb{Z}}$  generated at level  $j$ , two piecewise linear interpolants

$$\mathfrak{P}^j(x) = \frac{x - i2^{-j}}{2^{-j}} p_{i+1}^j + \frac{(i+1)2^{-j} - x}{2^{-j}} p_i^j, \quad i2^{-j} \leq x \leq (i+1)2^{-j}, \quad (7)$$

$$\mathfrak{N}^j(x) = \frac{x - i2^{-j}}{2^{-j}} n_{i+1}^j + \frac{(i+1)2^{-j} - x}{2^{-j}} n_i^j, \quad i2^{-j} \leq x \leq (i+1)2^{-j}. \quad (8)$$

**Definition 4.1.** A subdivision scheme refining point-normal pairs is termed convergent if the two sequences of functions  $\{\mathfrak{P}^j\}_{j \in \mathbb{Z}_+}$  and  $\{\mathfrak{N}^j\}_{j \in \mathbb{Z}_+}$  are uniformly convergent in the sup-norm.

Note that the definition above is in accordance with the definition of convergence of vector subdivision schemes [13].

The most important property of a scheme modified by BQA is stated in the next theorem.

**Theorem 4.2.** If a modified algorithm converges then it generates limit normals which are the normals of the limit curve.

*Proof.* Convergence of the algorithm implies the contractivity of the edges and of the angles between consecutive normals. Thus, as the algorithm progresses, the length  $|p_{i-1}^j p_i^j|$  ( $j$  is the index of iteration) becomes smaller, as well as the length of the tangents. So, the auxiliary Bezier curve from which we sample the BQA, approaches the segment  $[p_{i-1}^j p_i^j]$ , and the sampled normal becomes closer to the perpendicular of the segment.  $\square$

The next theorem gives a lower bound of the smoothness of curves generated by converging modified scheme.

**Theorem 4.3.** If a modified algorithm converges then it produces at least  $G^1$  smooth curves.

*Proof.* Convergence of the algorithm implies convergence of the normals. The limit curve has those normals, as we showed in Theorem 4.2. Namely, the limit curve has normals that changes continuously, which constitutes  $G^1$  smoothness.  $\square$

The fact that consistency "almost holds" for two PNPs sampled from the same circle, as stated in the previous section, leads to the following observation, similar to the one about the circle average in Section 3 of [11].

**Property 4.4.** Any modified subdivision scheme "approximately reconstructs" circles. Namely, if the initial PNPs are sampled from a circle, then the limit curve of any modified subdivision scheme is very close to that circle.

#### 4.1 Examples of modified schemes

For presenting the effect of our new quasi-averaging method, we chose the Lane-Riesenfeld algorithm and the 4-point scheme as the linear schemes to be modified. We term these two algorithms as MLR and M4Pt respectively. The two modified schemes are given in Algorithm 1 and Algorithm 2. We denote by  $MLR_i$ ,  $i = 0, 1, 2, \dots$  this variant of the modified Lane-Riesenfeld algorithm with  $i$  smoothing steps.

Here we provide several examples. In Figures 4, 5 we depict the limit curve and the limit normals. It is clear that the limit of the normals are the normals of the limit curve. In Figure 4 the original control polygon is a square and the normals are perpendicular to one of their adjacent edges. Note that the generated curves are without cusps. The result obtained in [1] by a similar construction lacks this property (see Table 1 there). Also note, that the result

---

**Algorithm 1** Modified Lane-Riesenfeld algorithm

---

**Input:**  $m \in \mathbb{N}_0$ ,  $P_i = (p_i, n_i)$ ,  $i \in \mathbb{Z}$ .

```
for  $i \in \mathbb{Z}$  do
   $P_i^0 \leftarrow P_i$ 
end for
for  $j=1,2,\dots$  do
  for  $i \in \mathbb{Z}$  do
     $P_{2i}^{j,0} \leftarrow P_i^{j-1}$ 
     $P_{2i+1}^{j,0} \leftarrow P_i^{j-1} \tilde{\odot}_{\frac{1}{2}} P_{i+1}^{j-1}$ 
  end for(i)
  for  $k = 1, \dots, m-1$  do
    for  $i \in \mathbb{Z}$  do
       $P_i^{j,k} \leftarrow P_i^{j,k-1} \tilde{\odot}_{\frac{1}{2}} P_{i+1}^{j,k-1}$ 
    end for(i)
  end for(k)
  for  $i \in \mathbb{Z}$  do
     $P_i^j \leftarrow P_i^{j,m-1}$ 
  end for(i)
end for(j)
```

---

of  $\text{MLR}_2$  seems to interpolate the data although it is not expected to do so, and that in (a) and (b) the curves are outside the input square.

Figure 5 demonstrates the editing capabilities of three algorithms. Every column shows curves generated from the same original control polygon but with one of the normals rotated.

---

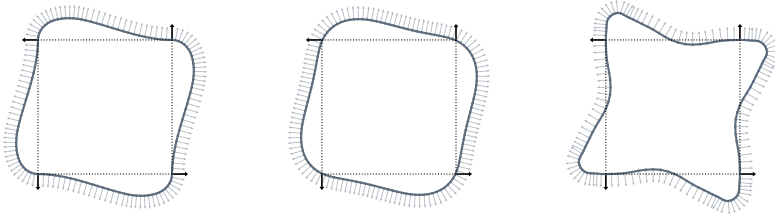
**Algorithm 2** M4Pt

---

**Input:**  $P_i = (p_i, n_i)$ ,  $i \in \mathbb{Z}$ .

```
for  $i \in \mathbb{Z}$  do
   $P_i^0 \leftarrow P_i$ 
end for
for  $j=1,2,\dots$  do
  for  $i \in \mathbb{Z}$  do
     $P_{2i}^j \leftarrow P_i^{j-1}$ 
     $S_L \leftarrow P_i^{j-1} \tilde{\odot}_{-\frac{1}{8}} P_{i-1}^{j-1}$ 
     $S_R \leftarrow P_{i+1}^{j-1} \tilde{\odot}_{-\frac{1}{8}} P_{i+2}^{j-1}$ 
     $P_{2i+1}^j \leftarrow S_L \tilde{\odot}_{\frac{1}{2}} S_R$ 
  end for
end for
```

---

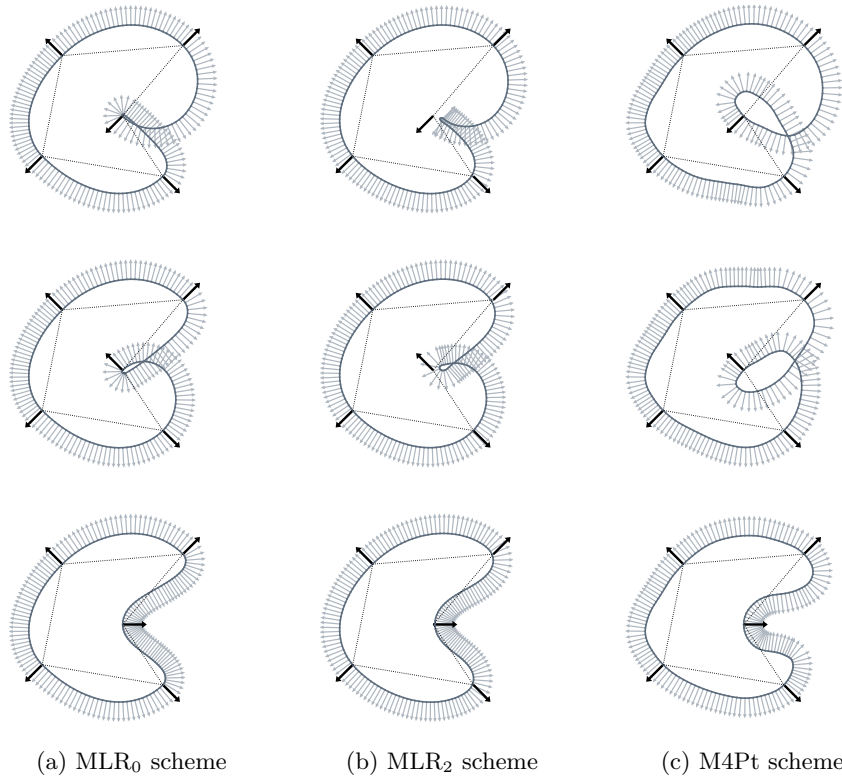


(a)  $\text{MLR}_0$  scheme

(b)  $\text{MLR}_2$  scheme

(c)  $\text{M4Pt}$  scheme.

Figure 4: Square input polygon with a special normal setup. Every normal is perpendicular to one of its adjacent edges. The limit curve and the limit of the normals are depicted.



(a)  $\text{MLR}_0$  scheme

(b)  $\text{MLR}_2$  scheme

(c)  $\text{M4Pt}$  scheme

Figure 5: Editing capabilities of  $\text{MLR}_0$ ,  $\text{MLR}_2$ ,  $\text{M4Pt}$ , starting from a generic polygon, due to changes in one normal. Each example depicts the initial polygon and normals, the limit curve and the limit normals.

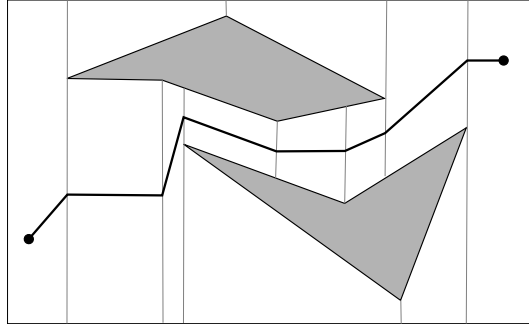


Figure 6: Typical point robot path.

## 5 Robot path smoothing

In this section we study the problem of smoothing a precomputed feasible polygonal path of a point robot. The input to the proposed solution is a feasible point robot path, given as a polyline. The output is a refined polyline, which is a piecewise linear approximation of a smooth curve. We present numerical values of discrete curvatures and of angles, and conclude the smoothness level of such a curve.

The approach in this section is based on the  $\text{MLR}_0$  algorithm. The main challenge of our approach is to avoid obstacles while keeping a certain level of smoothness. We achieve this by introducing an additional step in the averaging method. Our algorithm computes a curve, which is smooth in the areas with sufficient clearance and preserves the collision-free precomputed polyline in zero-clearance regions. Note that the proofs of Theorems 4.2 and 4.3 hold also in this setting.

### 5.1 Preliminaries

The solution presented in this work refines a precomputed feasible robot path. This path avoids obstacles, that we denote as  $\{o_i\}_{i \in \mathbb{Z}}$ . Each such obstacle is a polygon. We assume that the input path is obtained by the `ComputePath` algorithm of [2], or by similar ones. This algorithm first splits the free space into a set of trapezoids, and then computes the path. An important property of the path is that every edge of it is in a trapezoid, there is at most one boundary edge of an obstacle above the path segment and one below it. See [2] for explicit details and Figure 6 for an example of a typical scene.

### 5.2 Initial normals

In this section we describe a method for determining initial normals at the vertices of the given path. This method is proposed in [11]. We invoke it only in the initial step of the solution.

To compute the initial normals, we first attach to each edge of the path  $[p_i, p_{i+1}]$  a unit normal  $v_i$ , which is perpendicular to it, and satisfies  $v_i \times \overrightarrow{p_{i-1}p_i} > 0$ , so that  $v_i$  is to the left of  $\overrightarrow{p_{i-1}p_i}$ .

We determine a normal  $n_i$  at the vertex  $p_i$  as the weighted geodesic average of  $v_{i-1}$  and  $v_i$ , with weights

$$\frac{|p_{i-1}p_i|}{|p_{i-1}p_i| + |p_ip_{i+1}|}, \text{ and } \frac{|p_ip_{i+1}|}{|p_{i-1}p_i| + |p_ip_{i+1}|} \quad (9)$$

respectively. In case  $p_i$  is a boundary vertex, the normal is taken as that of the only neighboring edge.

### 5.3 Averaging method adapted to obstacles

Here we update the definition of the averaging method of Algorithm A, in Section 3. In particular, we change the tangent length  $\ell$ , defined in (1). The original value is motivated by a circle approximation. We sacrifice this property in favor of obstacles avoidance.

Let  $Tr_i$  be the trapezoid that the edge  $p_ip_{i+1}$  belongs to, and let  $Tr_i^u, Tr_i^b$  be the upper and the bottom bounding segments of this trapezoid respectively. We denote by  $L_i^u (L_i^b)$  the line defined by  $Tr_i^u (Tr_i^b)$ . Using the notation of Section 3, we obtain Algorithm B by introducing an additional step in Algorithm A.

**Step 4.1** Test, whether  $[c_0, c_1]$  ( $[c_2, c_3]$ ) intersects  $L_i^u$  or  $L_i^b$  of the trapezoid  $Tr_i$  corresponding to  $[p_0, p_1]$ . If there is an intersection then set  $c_1$  ( $c_2$ ) to be the intersection point nearest to  $c_0$  ( $c_3$ ).

See Figure 7 for two examples. In Figure 7a the intersection between  $[c_2, c_3]$  and  $L_i^u$  is inside  $Tr_i$ , while in Figure 7b the intersection between  $[c_0, c_1]$  and  $L_i^u$  is outside of the corresponding trapezoid.

We term  $MLR_B$  the Lane-Riesenfeld algorithm without smoothing steps ( $m = 1$ ) and with Algorithm B as the basic averaging operation.

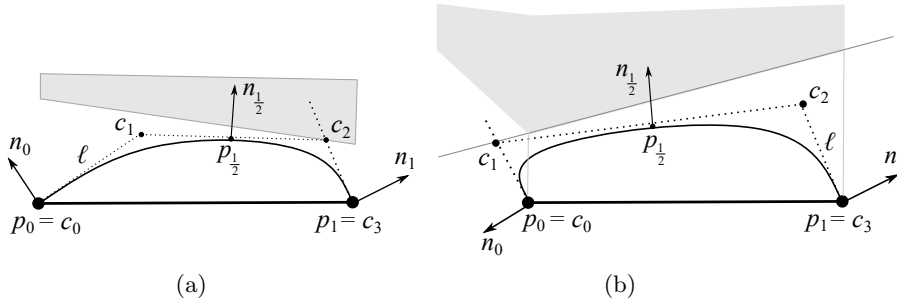


Figure 7: Computing  $P_{1/2}$  near an obstacle

**Theorem 5.1.** *A refined polyline generated by  $MLR_B$  with Step 4.1 is in the free space.*

*Proof.* For a given edge of the input path  $[p_i, p_{i+1}]$ , we know that  $p_i$  and  $p_{i+1}$  are in the free space. By construction, the corresponding  $c_1$  and  $c_2$  are in the free space as well as the entire  $[p_0, c_1]$  and the entire  $[c_2, p_1]$ . Also,  $c_1$  and  $c_2$  are in the same half-plane relative to  $L_i^u (L_i^b)$ . This guarantees that the entire  $[c_1, c_2]$  is in the free space too. Thus, the convex hull of  $c_0, c_1, c_2, c_3$  is in the free space. A Bezier curve is contained in the convex hull of its control points. This guarantees that the computed  $p_{1/2}$  is in a legal position as well.  $\square$

## 5.4 Measuring discrete smoothness

We present methods how to check the smoothness level of the obtained results.

For a refined polyline, we estimate the first derivative of the limit curve corresponding to the vertex  $p_i$  as

$$\gamma'_i = \frac{\mathbb{A}([p_{i-1}, p_i], [p_i, p_{i+1}])}{2^m}, \quad (10)$$

where  $m$  is the number of iterations that the  $\text{MLR}_B$  algorithm executes, and  $\mathbb{A}$  is the angle between two successive segments (the smaller angle between the two).

We estimate the curvature of the limit curve by computing the following values for every three successive vertices of the refined polyline:  $p_{i-1}, p_i, p_{i+1}$ . We find the circle that passes through these vertices, compute its radius  $r(p_{i-1}, p_i, p_{i+1})$ , and estimate the discrete curvature at  $p_i$  by

$$\check{\gamma}_i = \frac{1}{r(p_{i-1}, p_i, p_{i+1})}. \quad (11)$$

To study the properties of the smoothed path, we plot the graph of  $\{i, \gamma'_i\}_{i \in \mathbb{Z}}$ , and  $\{i, \check{\gamma}_i\}_{i \in \mathbb{Z}}$ . Values of  $\{\gamma'_i\}_{i \in \mathbb{Z}}$  close to zero indicate that the limit curve is  $C^1$ . Values of  $\{\check{\gamma}_i\}_{i \in \mathbb{Z}}$  with small fluctuations indicate that the limit curve is  $C^2$ .

## 5.5 Examples

In Figures 8 - 12 we depict several examples and comment on them. We perform four iterations of  $\text{MLR}_B$  in every example. In the left subgraph of each figure, we show the  $\gamma'$ -graph (orange) and the  $\check{\gamma}$ -graph (blue). Note, that all the  $\gamma'$ -graphs are in accordance with Theorem 4.3. In the right subgraph we show:

- o the obstacles (gray),
- o the initial path (green),
- o (optional), initial normals (green arrows),
- o the refined result (red)

In Figures 8 - 10 we present a scene with three obstacles and a zero-clearance corridor.

In Figure 8 the input path has 4 PNPs and does not pass through the zero-clearance corridor. The generated path consists of 49 points and its "curvature" fluctuates at few locations. Note that Step 4.1 is not invoked during the computation.

In Figure 9 the input path has 8 PNPs and passes through the zero-clearance corridor. The corresponding segment of the initial path is preserved. This straight part of the computed path is reflected as the zero segment in the curvature plot. Figure 10 is the same example, but the PNPs of the initial input are given in the reversed order. So, the curvature plot is "reflected", comparing with the example of Figure 9. In both examples the generated paths consist of

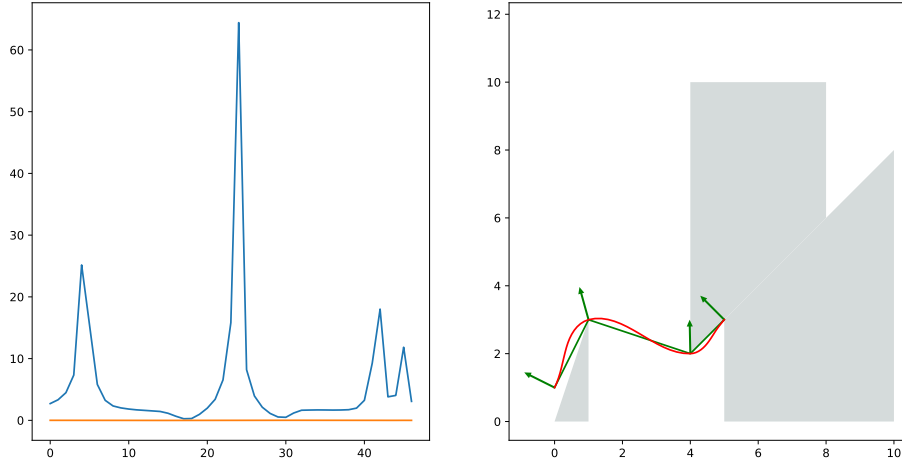


Figure 8: Simple case: Step 4.1 is not invoked.

113 points.

In Figure 11 we process the same input as in Figures 9, 10 but we add a close obstacle. Step 4.1 is invoked. Still, the algorithm preserves nice curvature behavior in the problem region.

Finally, in Figure 12, we study a scene with a remote obstacle. The algorithm does not use all the free space available for smoothing.

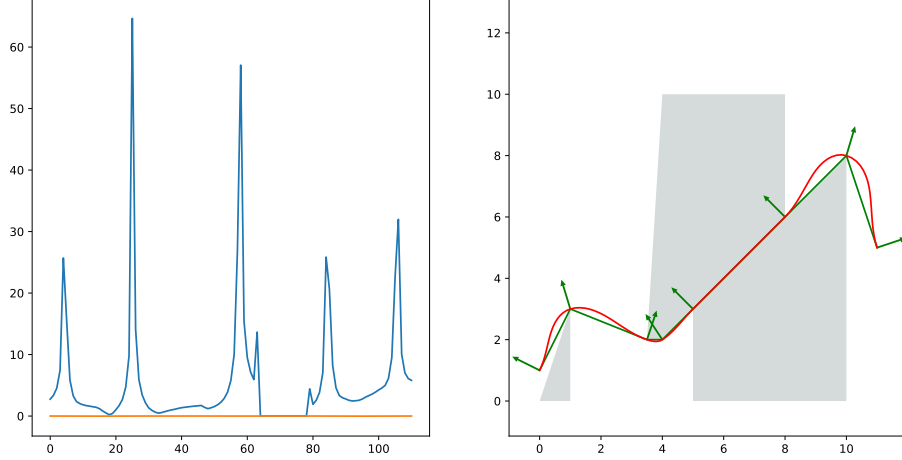


Figure 9: Zero clearance pass.

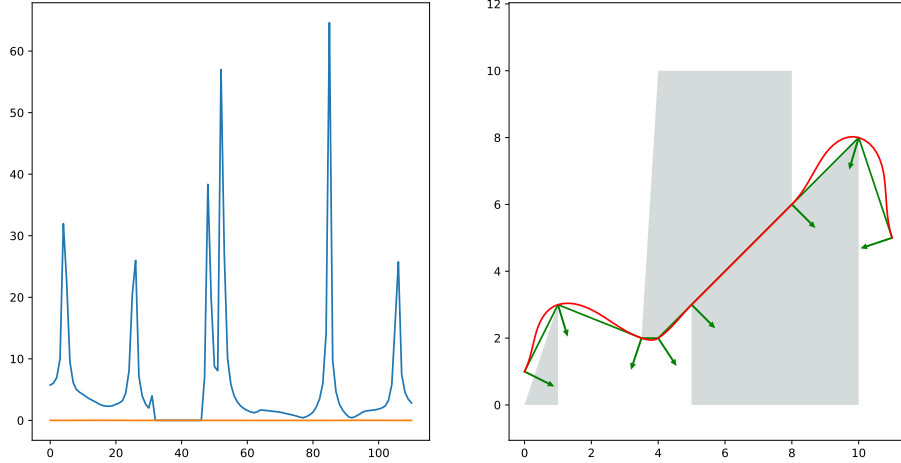


Figure 10: The reversed version of the previous example.

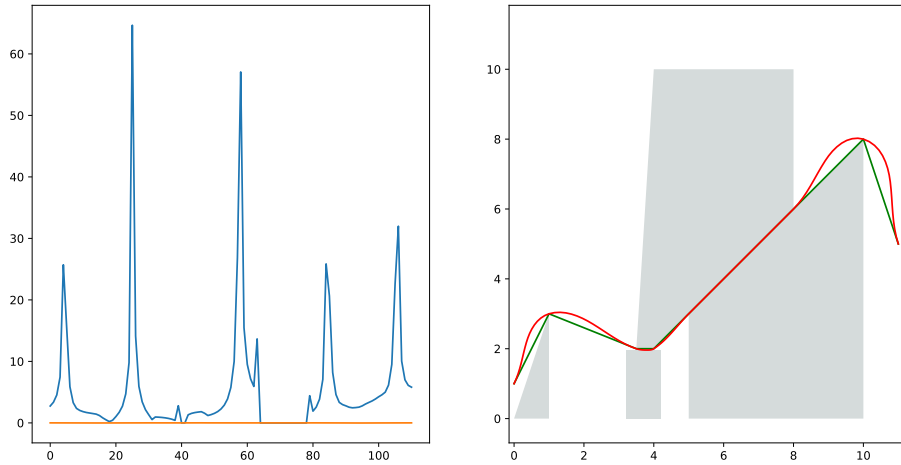


Figure 11: Adding a close obstacle.

## 6 Conclusions

We improve the method in [1] for the insertion of a PNP in between two PNPs, and use it as a quasi-average in subdivision schemes. We modify the Lane-Riesenfeld algorithm and the 4-point scheme with this new quasi-average. The limit normals generated by such a modified algorithm are the normals of the limit curve. We show examples, indicating that the presented modified algorithms extend the editing capabilities of typical CAGD and graphics systems.

We add Step 4.1 to Algorithm A, constructing the quasi-average, and apply the resulting  $MLR_B$  algorithm to smooth a feasible robot path, given as a polyline. We show that computing all tangent lengths by one formula, as is done in Algorithm A, is not mandatory. The curve, generated by  $MLR_B$ , is

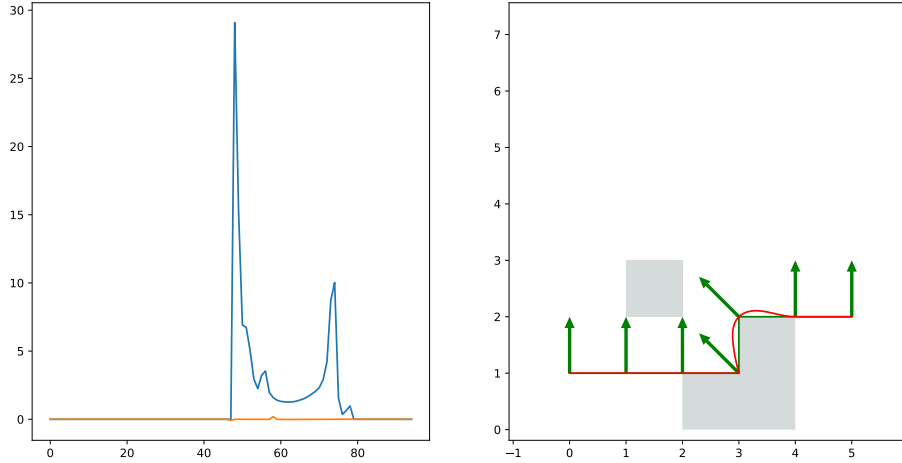


Figure 12: Poor utilization of the free space.

smooth enough away from the obstacles.

The implementation code of the presented algorithms in this paper can be found in our Github repository at <https://github.com/subdivision/BSubd>.

**Remark 6.1.** *While working on this paper, we tried different curves as candidates for an auxiliary curve to sample the quasi-average PNP from. We tested Bezier curves and B-spline curves of 3rd and higher degrees. For degrees higher than 3, we used `scipy` Python package. It appears that there is no gain over the use of cubic Bezier curves. The computed limit curves are barely distinguishable both visually and numerically (e.g. almost similar curvature plots). We prefer the cubic Bezier curves due to their closed formulas and faster computations. Still, investigating alternative auxiliary curves might be an interesting subject to research.*

## 7 Future work

We see several possible directions for future work.

To prove the convergence of the MLR and M4Pt schemes and to analyze their smoothness. To extend the quasi-average of two 2D PNPs to 3D PNPs, and to use it in modified subdivision schemes for surface generation. The latter is work in progress.

In Section 5 we reduce the tangent length in areas with insufficient clearance and keep the original value of  $\ell$  in areas with remote obstacles. An open question is: can a judicious choice of  $\ell$  at each location improve smoothness? A potential problem in this approach could be the fact that the use of values of  $\ell$  greater than the  $\ell$  in (1) might produce Bezier curves with self intersecting control polygon, which by Theorem 3.2 does not occur when  $\ell$  is given by (1).

## Acknowledgments

The author would like to thank Nira Dyn for fruitful discussions and useful comments that contributed to the quality of this paper.

## References

- [1] Mao Aihua, Luo Jie, Chen Jun, and Li Guiqing. A new fast normal-based interpolating subdivision scheme by cubic Bézier curves. *The Visual Computer*, 32(9):1085–1095, 2016.
- [2] Mark de Berg, Otfried Cheong, Marc van Kreveld, and Mark Overmars. *Computational Geometry: Algorithms and Applications*. Springer-Verlag TELOS, Santa Clara, CA, USA, 3rd ed. edition, 2008.
- [3] Pavel Chalmovianský and Bert Jüttler. A non-linear circle-preserving subdivision scheme. *Adv. Comp. Math.*, 27:375–400, 2007.
- [4] John Connors and Gabriel Elkaim. Analysis of a spline based, obstacle avoiding path planning algorithm. 2007.
- [5] Costanza Conti and Nira Dyn. Analysis of subdivision schemes for nets of functions by proximity and controllability. *Journal of Computational and Applied Math.*, 236:461–475, 2011.
- [6] Tor Dokken, Morten Dæhlen, Tom Lyche, and Knut Mørken. Good approximation of circles by curvature-continuous Bézier curves. *Computer Aided Geometric Design*, pages 33–41, 1991.
- [7] Nira Dyn and Elza Farkhi. Spline subdivision schemes for compact sets—a survey. *Serdica Math. J.*, 28 (4):349–360, 2002.
- [8] Nira Dyn and David Levin. Subdivision schemes in geometric modelling. *Acta Numerica*, 11:73–144, 2002.
- [9] Tobias Ewald, Ulrich Reif, and Malcolm Sabin. Hölder regularity of geometric subdivision schemes. *Constructive Approximation*, 42:425–458, 2015.
- [10] Martin Glöderer and Andreas Hertle. Spline-based trajectory optimization for autonomous vehicles with ackerman drive. 2010.
- [11] Evgeny Lipovetsky and Nira Dyn. A weighted binary average for subdivision schemes of point-normal pairs. *Computer Aided Geometric Design*, 48:36–48, November 2016.
- [12] Evgeny Lipovetsky and Nira Dyn.  $C^1$  analysis of some 2D subdivision schemes refining point-normal pairs with the circle average. *Computer Aided Geometric Design*, 69:45–54, 2019.
- [13] Charles Micchelli and Tomas Sauer. On vector subdivision. *Mathematische Zeitschrift*, 229:641–674, 1998.
- [14] Inam Ur Rahman, Iddo Drori, Victoria C. Stodden, David L. Donoho, and Peter Schröder. Multiscale representations for manifold-valued data. *Multiscale Model. Simul.*, 4(4):1201–1232, 2005.

- [15] Simon Thompson and Satoshi Kagami. Continuous curvature trajectory generation with obstacle avoidance for car-like robots. 2006.
- [16] Johannes Wallner and Nira Dyn. Convergence and  $C^1$  analysis of subdivision schemes on manifolds by proximity. *Computer Aided Geometric Design*, 22(7):593–622, 2005.
- [17] Aiwu Zhang and Caiming Zhang. Tangent direction controlled subdivision scheme for curve. *The 2nd Conference on Environmental Science and Information Application Technology*, 4, 2010.